Photoluminescence

Woojin Han[1]

[1]Seoul National University, Seoul 151-747, Korea

April 24, 2023

Abstract

1 Introduction

In this experiment, photoluminescence(PL) of ruby and rhodamine 590 is measured. Analysis between PL peak statics of ruby and temperature is obtained.(3.3) The effect by aperture of spectrograph to PL result is declared, and proved.(3.1) According to the peak intensity ratio, the mole ratio of Cr^{3+} ion in the ruby is calculated. The apparatus data () is also found and compared to the calculation.

1.1 Photoluminescence : General Theory

Photoluminescence is explained by two different parts, absortion and emission of light. Both events occur by the electronic transition through states, embedding the nature of the condensed matter. Therefore, the photoluminescence result lead us to measure the band diagram of the crystal. Not only the energy level of each band but also lifetime or exact orbital can be measured by the peak statics, such as peak width or intensity ratio.

Fig. 1(a) shows the band diagram explaination of light absortion, creating hole in lower band transite to upper band. Fig. 1(b) is the schematic diagram of light emission, slowly relaxing and emitting light while energy drops between band gap. Fig. 2 is one of the photoluminescence results in this experiment. The absorbed light was $532nm$, but we can find out the emitted light have wavelength around $690nm$. We can sure the electronic transition is the key mechanisms since the wavelength change can not be explained by scattering, especially for the peak nature. Therefore, the peak position is specific to the crystal structure or the molecular shapes. But the peak width have two reasons, natural and optical broadening. ([11]) Natural broadening is intrinsic to the transition, caused by lifetime of the states. For lifetime τ, the spectral function

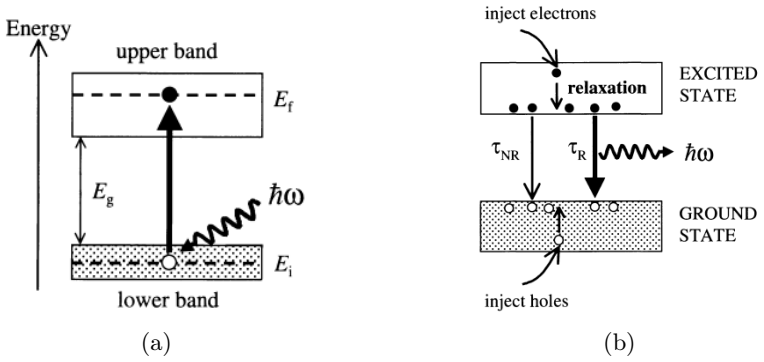

Figure 1: Schematic diagram of (a)light absortion (b)light emission [10]

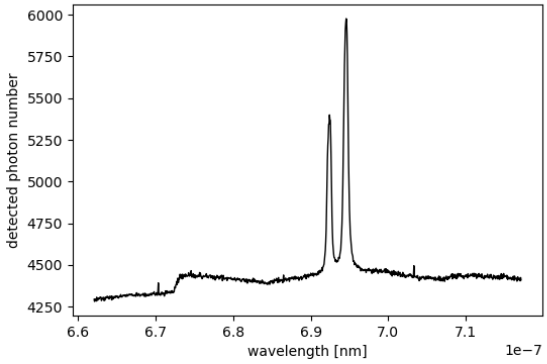

Figure 2: photoluminescence results of Ruby in $170.0K$

follows Lorentzian like equation (1), ω is the angular frequency of light, and $\Delta\omega$ is full width at half maximum(FWHM) value which is related with lifetime.

$$g(\omega) = \frac{\Delta\omega}{2\pi}\frac{1}{(\omega-\omega_0)^2+(\Delta\omega/2)^2},\ \Delta\omega = \frac{1}{\tau} \tag{1}$$

And by the spectral effects by spectroscopy itself, the Gaussian shape optical broadening is inevitable. Therefore, I assume that the detected photoluminescence spectroscopy data will follow Voigt profile, which is a convolution results of Lorentzian and Gaussian function.

1.2 Ruby

In the theory of solid state luminescence, simultaneous emission is allowed between special states. Otherwise, electron can loses its energy in phonon which we call nonradiative transition. The phonon physics is explained by debye

model, assuming that the highest frequency of phonon is restricted by the size of the lattice denoted as ω_D. And phonon follows boson statics, can easily induces the density of states.

$$H = \sum_{n=0}^{3} \epsilon_n \psi_n^\dagger \psi_n + \sum_k (\hbar\nu k)(a_k a_k^\dagger + \frac{1}{2}) + S_0(C_{12}\psi_1^\dagger + \sum_{n=1,2} C_{n3}\psi_n^\dagger \psi_3 + c.c.) + S_0^2(\sum_{n=0}^{2} d_n \psi_n^\dagger \psi_n + [d_{12}\psi_1^\dagger \psi_2 + c.c.]) \quad (2)$$

In [7], they declare the phenomenological Hamiltonian of impurity ruby as equation 2. As the two big peak is observed near $690nm$, we assume three excited-state levels $n = 1, 2, 3$ have energy of $\epsilon_1, \epsilon_2, \epsilon_3$ and wave function of ψ_1, ψ_2, ψ_3 respectivly. The first term is about the impurity electronic states energy. The second term is phonon energy, which k is bounded by Debye frequency. In ruby, first and second excited states are E_2 levels and the photoluminescence peak appears by the spontaneous emission through $1 \to 0$ and $2 \to 0$. Empirically, $0 = \epsilon_0 << \epsilon_1 < \epsilon_2 << \epsilon_3$, since the gren laser excites electron by $0 \to 3$ and by nonradiative $3 \to 1, 2$ transition occurs. The leftover terms are suggested perturbation term in [7], assuming the dopped Cr^{3+} locates isotropic in enlarged Debye-model. In this experiment, the dopped ratio is small enough to fit in the assumption.

$$\epsilon_n(T) = \epsilon_n(0) + \alpha_n(\frac{T}{T_D})^4 \int_0^{T_D/T} dx \frac{x^3}{e^x - 1} - \beta_{12}(-1)^n \frac{T_e}{T_D}(\frac{T}{T_D})^2 \times \int_0^{T_D/T} dx \frac{x^3}{e^x - 1} \frac{P}{x^2 - (T_e/T_D)^2} \quad (3)$$

$$\Gamma_n(T) = \Gamma_n(0) + \bar{\alpha_n}(\frac{T}{T_D})^7 \int_0^{T_D/T} dx \frac{x^6 e^x}{(e^x - 1)^2} + \pi\beta_{12}(\frac{T_e}{T_D})^3[\delta_{n2} + \frac{1}{e^{T_e/T} - 1}] \quad (4)$$

After calculating lowest order of perturbation theory, we have the peak position in function of temperature as equation 3. T_D is Debye temperature, α_n, β_{12} is fitting coefficients, $T_e = (\epsilon_2 - \epsilon_1)/k_B$ is $42K$ in ruby. Equation 4 shows the temperature dependance of each peak width, Γ denotes the parameter of Lorentzian lineshape. $\bar{\alpha_n}$ is also a fitting variable, which have direct expression to hamiltonian coefficients. The first temperature perturbed term starting with $\alpha_n, \bar{\alpha_n}$ in both equation is a calculation of nonradiative effects. The second term starting with β_{12} is the term of internal conversion between state $1, 2$. In this case, the internal conversion can be disregarded, $\beta_{12} = 0$. Specific fitting method and results in this experiment are denoted below. (3.3)

Those explaination doesn't imply the specific states, since we never comes out with the crystal environments. Ruby is dopped crystal which basic structure is built by Al_2O_3, hexagonal crystal structure, Cr^{3+} located in octahedral site. In this case both crystal and ion energy state affect themselves to have broad band structure or energy splits. Al_2O_3 doesn't have any fluorescence bandgaps, since we can never find photoluminescence peaks on other dopped ions. Which means that the affected Cr^{3+} energy structure is the key of this luminescence effects. Fig 3, adapted from [3] shows the shift of ioninc energy structure. The left side of the diagram is the original orbital energy of free Cr^{3+}. As the cubic field parameter Dq/B increases, the energy level splitted and broadened. The diagram at $Dq/B = 3$ represents energy level of the Cr^{3+} in ruby, which doesn't splitted enough and considered as constant. So, ${}^4A_2, {}^2E, {}^2T_1, {}^4T_2$ is the $\epsilon_0, \epsilon_1, \epsilon_2, \epsilon_3$ state respectivly as explained. As a conclusion, the dopped ruby absorb green light to transite electron from ${}^4A_2 \rightarrow {}^4T_2$ and nonradiative transite to ${}^4T_2 \rightarrow {}^2T_1, {}^2E$ and give R_1, R_2 emitted light peak by ${}^2T_1, {}^2E \rightarrow {}^4A_2$.

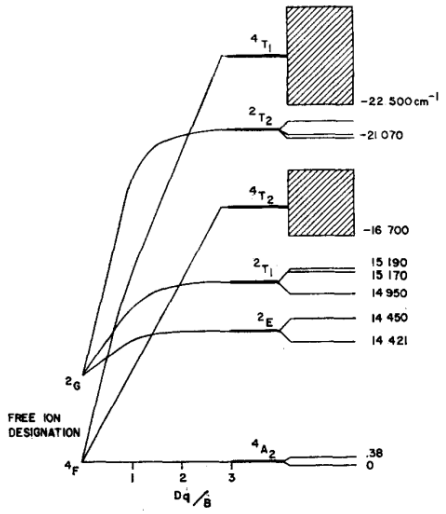

Figure 3: Energy level diagram of Cr^{3+} in ruby. adapted form [3]

1.3 Rhodamine 6G(R6G)

Rhodamine 6G (R6G) is one of the highly fluorescent triarylmethane dyes. Fig. 4 shows the molecular structure of R6G. It has three benzene ring, which allows each atomic orbital forms fluorescence cojugated system. In photochemistry, we assumes the linear combination of each atomic orbitals form molecular orbital. Which means that, the total hamiltonian of molecule is described by the function of linear coefficients. Therefore, eigenstate of the hamiltonian gives the energy diagram of a molecule. In this experiment, we dissolve R6G in ethylene glycol, which need different approach to ruby. Since the molecules does not fixed

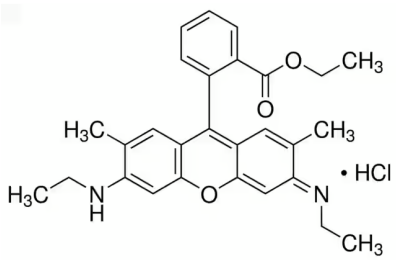

Figure 4: Structural formula of R6G, adapted from [9]

by its position, it can freely vibrate and rotate. Therfore, the PL results of R6G must consider a Raman shift. And also [5] reports that the concentration of the solution effects the peak position and FWHM. It declares a significant role of dimer formation by $\pi - \pi$ stacking interaction. But by Frank condon principle, the molecular position does not change while electric transition occurs, the energy gap between monomer and dimer is disregarded.

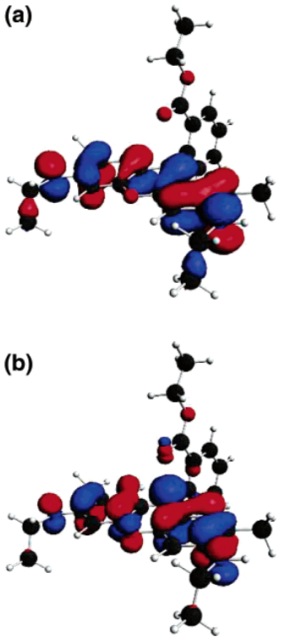

Figure 5: The HOMO (a) and LUMO (b) of R6G adapted from [6]

In photochemistry the nonradiative, and radiative transition can be explained once in Jablonski diagram. Jablonski diagram have each vibrational modes in multiplicity of states, denoted by $M = 2S + 1$. S is total electric spin. For example, if the all electron is in spin pair, $S = 0, M = 1$. It is singlet state.

By the value of $M = 1, 2, 3, 4, ...$ the state will named after singlet, doublet, triplet and so on. The state ${}^4S$ is fourth excited state of singlet. Fig. 5 shows highest occupied molecular orbital (HOMO) and lowest unoccupied molecular orbital (LUMO) of R6G molecule. By definition, as the light irradiates to the molecule electron excites over LUMO from HOMO. And, by nonradiative transition bring down the excited electron to LUMO, the radiative transition between LUMO and HOMO makes luminescence. As Fig. 5, each Benzene ring switches its phase have energy gap near 560nm. The photoluminescence transition is ${}^1S \rightarrow^0 S$, spin unchange transition.

2 Methods

Photoluminescence module has set up in intermediate physics experiment laboratory, Seoul National University. Laser is from Shanghai Dream Lasers Technology Co., Model is SDL-532-030T ([2]), maximum power of $30mW$ and low noise feature. Compressor is from CSIC Pride (Nanjing) Cryogenic Technology Co., Model is KDC 2000F ([1]) CCD camera is from Andor, Model is DV401A-BVF ([4]), which secures 99% linearity of photon detection. Spectrograph is from Dongwoo Optron Co., Model is MonoRa500I ([8]). Spectrograph has four slit, two of them were closed. Its slit can modified by the micrometer attached to each entrance. The modification is limited to open up an aperture, not the specific details of the spectrograph. Fig. 6(a) shows breif structure of the spectrograph. In this experiment, I close the left aperture by setting the dial to $-0.1mm$. The black arrow is the path of a laser in Fig. 6(b). The laser emitted from below splitted by dichroic filter, encounters to sample. Sample scatters light to every direction, but the diagram only shows the useful light ray which goes into the Notch filter. Each dichroic filter and Notch filter selects appropriate wavelength to each sample. I measures R6G soluted in ethylene glycol and ruby in room temperature, stantard pressure.

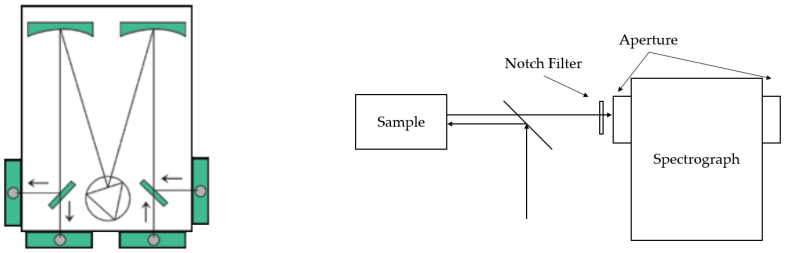

(a) (b)

Figure 6: Schematic diagram of (a) spectrograph, adapted form [8] (b)total photoluminescence module

2.1 Ruby : PL by temperature

I fix the alignment and set the sample pressure under 10mTorr using rotary pump. Then using compressor, lower the sample temperature from $270K$ to $10K$. If the grating speed is too fast, turn on the heater attached to sample to mediate the speed. I detect photons from CCD camera for every $5K$, and read the middle temperature of detection while proceeding. In this experiment, about $0.2K$ has cooled so the photoluminescence by temperature detection is vouched by accuracy of $0.1K$.

3 Results and Discussion

All of the results are uploaded at [14]. In this report some sample plots are attatched, which does not influence generality of logical flows. The file name and detailed contents are table at Fig. 7

file name	details
`Ruby sx-y_raw_fig.png`	Ruby PL plot of slit width x in repeated index y
`R6G(x)_raw_fig.png`	R6G PL plot of repeated index x, raw figure
`R6G(x)_gaussian_fitted_fig.png`	R6G PL plot of repeated index x gaussian fitted figure
`Ruby(T)_raw_fig.png`	Ruby PL plot in temperature T , raw figure
`Ruby(T)_voigt_fitted_fig.png`	Ruby PL plot in temperature T, voigt fitted figure
`R6G_total_fig.png`	United plot of R6G sample
`Ruby_temperature_peak_fig.png`	United plot of Ruby sample, peak position statics
`Ruby_temperature_width_fig.png`	United plot of Ruby sample, peak width statics

Figure 7: file appendix of [14]

3.1 Aperture setting

I repeatly measure ruby sample in same temperature, pressure and alignment condition, only changing the aperture slit width. Fig. 8 shows two extreme case of $0.05mm$ and $0.30mm$ opened results. As the aperture closed, less photon are detected, the peaks doesn't dominate the results. But, the widely opened aperture makes resolution worse. In this trade off we choosed to take slit width of $0.25mm$, since the Stokes sideband are significantly observable from that width. Which leads us to expect the minor band can be visable through the noise either.

3.2 Rhodamin 6G

Fig. 9(b) shows counts - energy $[eV]$ plot and its gaussian trend line. Peak statics of five repeated detection is provided at Fig. 10. $N(E) = A\frac{1}{\sigma\sqrt{2\pi}}e^{-\frac{1}{2}\frac{(E-E_0)^2}{\sigma^2}}$ values are obtained. The amplitude A and background light C does not inform

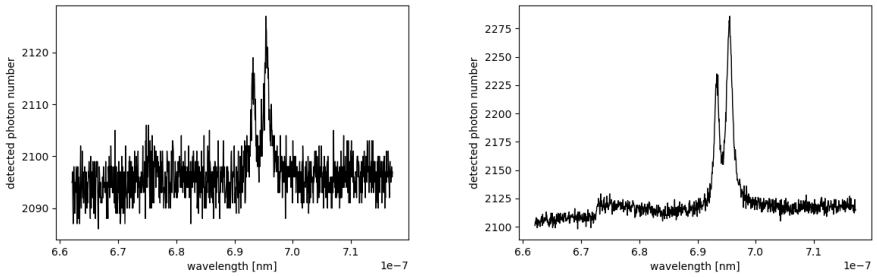

(a) (b)

Figure 8: PL result of ruby in (a)0.05mm (b)0.30mm opened aperture

a critical phenomena for R6G, the peak position and FWHM only matters. The band gap betwen LUMO and HOMO is 2.211 ± 0.001 $[eV]$ and its lifetime is $(7.15 \pm 0.02) \times 10^{-15}[s]$.

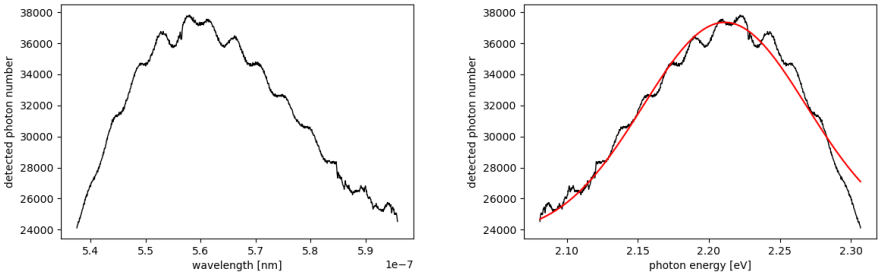

(a) (b)

Figure 9: PL result of R6G (a)counts - wavelength$[nm]$ (b)counts - photon energy$[eV]$

index	$E_0[eV]$	σ $[eV]$	A	C
1	2.211	5.78×10^{-2}	1.99×10^3	2.36×10^4
2	2.211	5.77×10^{-2}	2.10×10^3	2.47×10^4
3	2.211	5.77×10^{-2}	1.92×10^3	2.30×10^4
4	2.211	5.77×10^{-2}	2.03×10^3	2.41×10^4
5	2.211	5.76×10^{-2}	2.06×10^3	2.45×10^4

Figure 10: Statics of Gaussian fitting of Fig. 9 in different trials

The bumps on the peak is not a random error, but keep appears in repeated

measurements. Fig. 11(a) is the total plot of every datum in one plot. We can check that exactly same sidebands are at same position in different experiments. I have rotated the vials and moved the solutions position during the experiment, it does not have relation with outer variables. Therefore, I assumes those sideband are related with Raman scattering. The Raman shift of R6G has calculated in [6]. As the molecule in solution moves freely in ethylene glycol, the cross section of the band gap might Raman shifted. There are around 10-12 big peaks on raman shift as shown in Fig. 11(b), which is exactly same numbers to the experimental data. Also, the dimer effect has reported from [5], but in this experiment the solution is diluted enough to ignore the dimer effects.

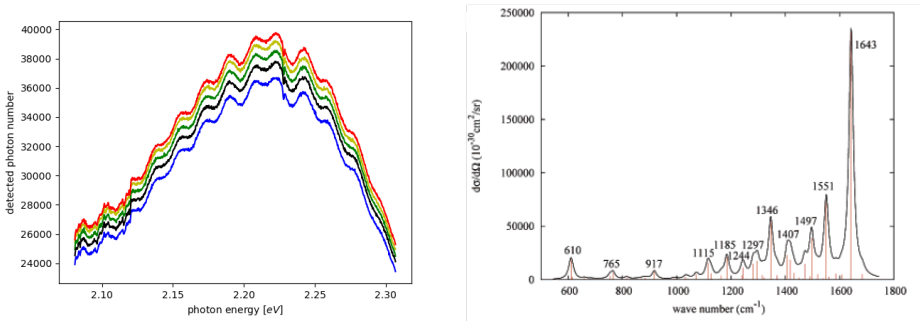

(a) (b)

Figure 11: (a)United plot of R6G PL data each color are the repeated measurements. (b)Raman shift calculation adapted from [6]

3.3 Ruby PL result by temperature

PL data of ruby for 51 different temperature is measured. Fig. 12 shows four representative PL plots of temperature 260.0, 190.0, 100.0, 6.00 K, 6.0mTorr. As the sample temperature went down, the peaks get sharper, and can find the subtle peak position shift. Unlike the left peak, R1 peak, the right peak, R2 peak get smaller so that at 6.0K, R2 peak is hard to find in noises. The fitting eqauation $N(E) = A_1 V(E - E_1; \sigma, \gamma_1) + A_2 V(E - E_2; \sigma, \gamma_2) + C$, where $V(x; \sigma, \gamma)$ is Voigt profile. Fitting parameters are E_1 R1 peak position, γ_1 R1 peak Lorentzian FWHM and A_1 is the total photon number of R1 peak. Same definition belongs to R2 peak. And σ is the Gaussian variance coefficient, which must be same for both peak. At extremely low temperature, R2 peak is gone so those values are fitted by one Voigt profile, and R2 peak statics setted NaN value. As this fitting assumes that the spectrograph errors are calculated in the parameter σ, the $\sigma[eV]$ to sample temperature does not have any relations. Unfortunately the optical broadening, σ is not equal to each temperature, but have some tendency with temperatures. I think that Voigt function fitting is

very frajile to have a lot of optimized parameter, so that σ have dependacy with sample temperature. Although it is totally fine since Voigt profile is normalized itself so that the amplitude directly means the peak area.

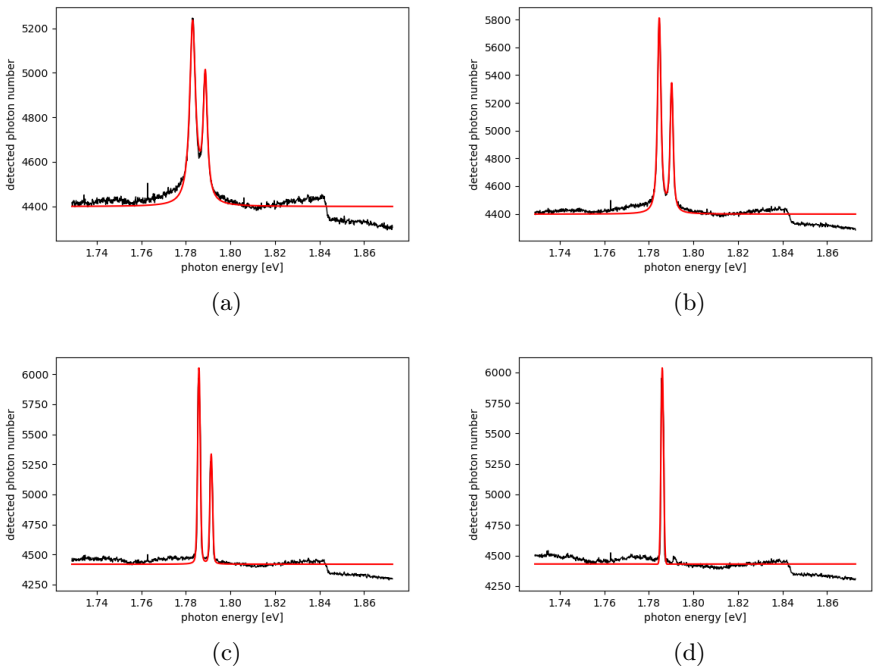

Figure 12: Ruby PL data of pressure 6.0mTorr, and temperature (a)260.0K (b)190.0K (c)100.0K (d) 6.00K, in count - energy $[eV]$ scale and its voigt fitting results (red)

Fig. 13 shows the temperature dependance of each peaks, error bar are attached to each data point. The error is propagated from the ccd camera resolution, every energy detection should have measurement error of 0.0001 $[eV]$. The error from fitting calculation have order of 10^{-10} $[eV]$, which are very small. By using equation 3 and 4, $\epsilon_n(0)$ and α_n, $\Gamma_n(0)$ and $\bar{\alpha_n}$ are fitted. As the assumption from [7], internal conversion coefficients β_{12} has been disregarded as 0. And also, Debye temperature T_D can calculated from the specific heat of $\alpha - Al_2O_3$ which is $760K$. Therefore, the peak positions at $0K$ are 1.7861 ± 0.0001, $1.7916 \pm 0.0001[eV]$.

Peak width is not clear enough, since Voigt profile is duplicates by various values of γ and σ. And, the Stokes sideband makes fitting goes to local optimal parameters, not the exact value of it. So, I suggest to use modified width defined by $\gamma^2 + \sigma^2$. With assertion that those value doesn't change a lot since $\sigma \ll \gamma$ holds. Therefore, the peak widths at $0K$ are $(5.6 \pm 0.5) \times 10^-4$, $(5.5 \pm 0.5) \times 10^-4$

$[eV]$. The lifetime of ${}^{T}_{1} \rightarrow^{4} A_2$ is 7.6×10^{-11} s, ${}^{2}E \rightarrow^{4} A_2$ is 7.7×10^{-11}s each. Those lifetime has order of $10^{-}11$ s, which is appropriate for luminescence transition.

$\alpha_1 = -0.0928 \pm 0.0001$, $\alpha_2 = -0.0875 \pm 0.0001$ $[eV]$, $\bar{\alpha_1} = 0.3275 \pm 0.0001$, $\bar{\alpha_2} = 0.1901 \pm 0.0001$ $[eV]$ values are also fitted. Those values have information of Cr^{3+} impurity values by calculation of [13]. Unfortunately, the experimental results by α_n to impurity is not available since modifying impuritiy of ruby crystal is too hard. So, in this report I use significant approach to calculate Cr^{3+} doping mole fraction in 3.4

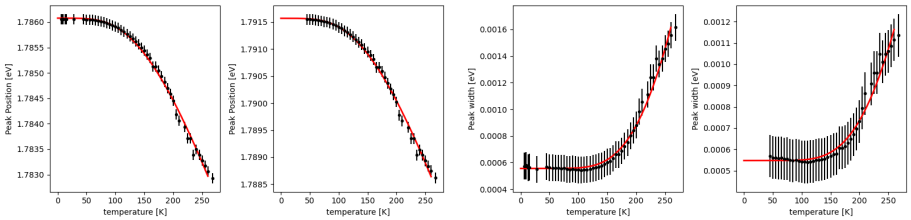

(a) (b)

Figure 13: (a) peak position $[eV]$ (b) peak width $[eV]$ to sample temperature [K] plot. R1(left), R2(right), red lines are the appropriate fitted functions.

3.4 Peak Height : dopped impurity

In [12]

4 Summary

References

[1] CSIC Pride (Nanjing) Cryogenic Technology Co. Kdc 2000f. http://www.724pridecryogenics.com/en/uploadfile/product/20180531112902906l1.pdf.

[2] Shanghai Dream Lasers co. ltd. Sdl-532-030t. http://www.dreamlasers.cn/products/laser/Low%20Noise%20Lasers.htm.

[3] Joseph A. Calviello Edward W. Fisheer and Zindel H. Heller. Direct t-e phonon relaxation in ruby and its effect upon r-line breadth.

[4] Oxford instuments. Andor idus 401 specifications. https://andor.oxinst.com/assets/uploads/products/andor/documents/andor-idus-401-specifications.pdf.

[5] I T Sugiarto Isnaeni and K Y Putri. Analysis of dual peak emission from rhodamine 6g organic dyes using photoluminescence.

[6] Lasse Jensen and George C. Schatz. Resonance raman scattering of rhodamine 6g as calculated using time-dependent density functional theory.

[7] D. E. McCumber and M. D. Sturge. Linewidth and temperature shift of the r lines in ruby.

[8] Dongwoo optron. Monora 500i. http://www.dwoptron.com/yc/data/item/1467027407/Monochromator.pdf.

[9] sigma aldrich. Rhodamine 6g. https://www.sigmaaldrich.com/KR/ko/product/aldrich/252433.

[10] someone. blah.

[11] someone. blah.

[12] Takeshi Shigenari Taro Toyoda, Takashi Obikawa. Photoluminescence spectroscopy of cr^{3+} in ceramicc $a1_2o_3$. *materials Science and Engineering B54*, 1998.

[13] J. H. Van Vleck. Paramagnetic relaxation times for titanium and chrome alum. *Phys. Rev.*, 57:426–447, Mar 1940.

[14] WoojinHan24. Photoluminescence. `https://github.com/WoojinHan24/Photoluminescence/tree/master/results`.